American Journal of Industrial Engineering, 2025, Vol. 9, No. 1, 1-7
Available online at http://pubs.sciepub.com/ajie/9/1/1
Published by Science and Education Publishing
DOI:10.12691/ajie-9-1-1

Adsorptive Removal of Basic Blue 9 by γ-Al_2O_3-based Kaolinitic Clay: Parametric, Kinetic and Equilibrium Studies

Gustave Tchanang[1,2,*], Jean M. Kepdieu[2], Kalaya Goumou[1], Mamadou Y. Baldé[2,3], Cyprien J. Ekani[2], Chantale N. Djangang[2], Phillipe Blanchart[4]

[1]Department of Chemistry, University Julius Nyerere of Kankan, Kankan, Guinea
[2]Department of Inorganic Chemistry, University of Yaoundé I, Yaoundé, Cameroon
[3]Department of Chemistry, University Gamal Abdel Nasser of Conakry, Conakry, Guinea
[4]Institute of Research on Ceramics of Limoges, University of Limoges, Limoges, France
*Corresponding author: tchanang.gustave@yahoo.com

Received May 15, 2025; Revised June 17, 2025; Accepted June 25, 2025

Abstract Experimental and theoretical investigations related to the adsorptive removal of Basic blue 9 (BB9) onto γ-Al_2O_3 (gamma-Nano alumina) have been done in the present work. Batch tests were carried out varying some processing parameters namely initial dye concentration (5 - 50 mg/L), adsorbent dose (0.5 - 5 g/L), initial pH (1 - 12) and contact time (0 - 30 min). Under conditions of C_0 = 50 mg/L; pH = 11; dose = 1g/L and t = 15 min, more than 83.6% of the BB9 molecules were removed corresponding to an adsorption capacity of 41.8 mg/g. The pseudo-second order and the Langmuir models fit well the experimental data with highest R^2 values of 0.99 and 0.91 respectively and lowest values of χ^2. This suggests adsorption process as limiting step on a homogeneous distribution of active sites on the adsorbent surface. The first step of adsorption mechanism involved electrostatic interactions between the negatively charged γ-Al_2O_3 surface in basic medium and secondly electrophilic-nucleophilic interactions. Compared to other adsorbents, γ-nano Al_2O_3 obtained in this work could be a good alternative for treatment water containing dye BB9.

Keywords: *γ-Nano alumina, Basic Blue 9, Adsorption, Equilibrium, Kinetic and mechanism*

Cite This Article: Gustave Tchanang, Jean M. Kepdieu, Kalaya Goumou, Mamadou Y. Baldé, Cyprien J. Ekani, Chantale N. Djangang, and Phillipe Blanchart, "Adsorptive Removal of Basic Blue 9 by γ-Al_2O_3-based Kaolinitic Clay: Parametric, Kinetic and Equilibrium Studies." *American Journal of Industrial Engineering*, vol. 9, no. 1 (2025): 1-7. doi: 10.12691/ajie-9-1-1.

1. Introduction

The water quality is a very important factor that determines healthy conditions of all aquatic ecosystems. The latter is continuously polluted by coloured products from human activities, such as colour photography, the cosmetics industry, the pharmaceutical and medicinal sectors, papermaking, hair products, agricultural research, chemical and biological research as well as photoelectric cells [1,2]. Man-made Industries release a large scale of coloured chemicals into receiving waters, which lead to their pollution and poses a danger to the environment. The consequences of this pollution in terms of human health include kidney dysfunction, problems with the reproductive system, liver and brain [3,4]. Moreover, these highly visible dyes influence aquatic life by reducing light penetration having a drawback on photosynthesis. Methylene blue (BB9) is a dye widely used in dyeing, cotton and tannin printing, but also in the medical context as an antiseptic. Its stability due to the inner aromatic ring is not favourable to its biodegradation [5,6]. The removal of such dyes with health dysfunctions on human health as diarrhea, nausea, cyanosis, skin irritations, eye burns from industrial waters is of great interest [1,7]. Several depollution methods such as photochemical degradation, coagulation, chemical oxidation, reverse osmosis, flotation and adsorption [8,9] have been investigated by several authors. The adsorption method is the most widespread and exploited because of its facile implementation, cost-effectiveness and efficiency, but above all its ability to separate a varied range of dye. Adsorption is a process of accumulation of an adsorbate on the surface of adsorbents such as resins, composites, mineral materials and activated carbon [7,8,10]. Thanks to its porous and chemical characteristics, but above all to its large specific surface area and adsorption capacity, activated carbon has been widely used as an adsorbent. However, the cost of manufacturing as well as reusability remains high.

Clays and clay-based materials and related extracts as alumina are considered as alternatives low-cost materials. Large beads alumina has been used by several workers with surface modification with ionic surfactants or not in other to adsorb both organic and inorganic pollutants. The nanoscale size may enhance the properties of the particles without any surface modification. This has been tested with satisfaction by some workers but with different adsorbates as phosphates, congo red and azodyes [11,12,13]. Nevertheless, few works using chemicals reactants to synthesize nano alumina and evaluating its efficiency in BB9 adsorption have been reported [14,15,16]. However, starting materials and synthesis procedures may influence the adsorptive properties of alumina nanoparticles. It seems interesting in this work to investigate the efficiency of γ-Nano alumina previously synthesized using a low-cost kaolinitic clay [17] in the adsorption of BB9 from aqueous solution. On the same line, the influence of some processing parameters including initial dye concentration, contact time, adsorbent dose and solution initial pH, as well as kinetics and equilibrium are to be investigated.

2. Materials and Methods

2.1. Materials

2.1.1. Adsorbate

An analytical grade BB9, purchased from PROLABO was used without any further purification. From a stock solution of 50 mg/L, several solutions with desired concentrations were prepared by dilution with distilled water.

The physical appearance and chemical structure of BB9 is shown in Figure 1.

Figure 1. Physical appearance of (a) Basic Blue 9 and (b) topological chemical structure

2.1.2. Adsorbent

γ-nano alumina powder (Na-Kc) used in this study was synthesised and characterized in a previous work [17]. It was extracted following a sol-gel method from kaolinitic clay treated at 700 °C to gain more reactivity. It was found to be an amorphous and porous material with a specific surface area of 146.8 m^2/g.

2.2. Methods

2.2.1. Adsorption Experiments

The adsorption of BB9 onto Na-Kc was investigated by varying parameters such as initial concentration, contact time, adsorbent dose and initial pH in a batch system. In each Erlenmeyer flask containing 20 mL of BB9 at different initial concentrations (5 to 50 mg/L), 0.02 g of Na-Kc was introduced and the mixture was kept stirred at a speed of 250 rpm at 28 °C and pH = 11 for contact times ranging from 0 to 30 min. The equilibrium time and the effect of the initial concentration of BB9 were studied at this phase. The influence of the initial pH and the adsorbent mass was studied for values ranging from 1.0 - 12.0 and 0.5 to 5 g/L respectively. The concentration of the BB9 dye prior to adsorption was determined using a UV-Vis spectrophotometer (Spectro Direct AQUALYTIC), at an absorbance wavelength of 669 nm. At the end of each adsorption process, the filtrate was separated and the concentration of the dye was assessed. Figure. 2 illustrate the calibration curve of the BB9 dye plotted by performing a series of dilutions.

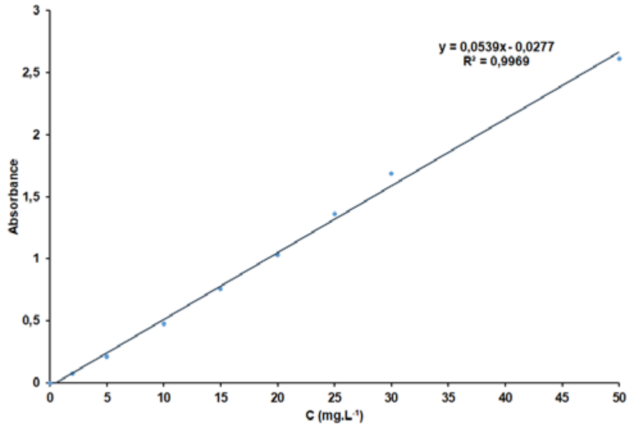

Figure 2. Calibration curve of BB9 dye

2.2.2. Theoritical Study

Adsorption capacities and Percentage removal

Equations (1) and (2) were used to determine the amount of dye adsorbed and the percentage of dye removal was calculated using equation (3).

$$q_t = \frac{(C_0 - C_t).V}{m} \quad (1)$$

$$q_e = \frac{(C_0 - C_e).V}{m} \quad (2)$$

Percent removal

$$(\%) = \frac{(A_0 - A_t)}{A_0} \text{ x } 100 \quad (3)$$

Where C_0, C_t and C_e are the initial, time t (min), and equilibrium dye concentrations (mg/L), respectively. V is the volume of solution (L) and m is the mass of adsorbent used (g). q_t and q_e (mg/g) are the adsorbed amount of BB9 per gram of adsorbent at time t and at equilibrium respectively.

Modeling and calculations related to kinetics and equilibrium have been done using models and techniques that are constantly in use, such as Langmuir and Freundlich for isothermal models and pseudo-first-order, pseudo-second-order, and intraparticle diffusion for kinetic models.

2.2.3. Isotherm Models

The Langmuir isotherm provides information regarding the availability of active sites on the adsorbent surface and the saturation of these sites once all the available sites are occupied and maximum adsorption is attained. The related non-linear equation is given by Eq. (4).

$$q_e = \frac{Q_m k_L c_e}{1 + k_L c_e} \quad (4)$$

Where q_e is the quantity of adsorbate fixed at equilibrium, Q_m is the maximum adsorbed quantity, Ce is the Concentration at equilibrium and K_L is the Langmuir constant depending on the nature of the solution, the temperature and the adsorbent surface.

The Freundlich isotherm has been established empirically for energetically inhomogeneous surfaces. The corresponding non-linear equation is presented in Eq. (5).

$$q_e = K_F Ce^n \quad (5)$$

With K_F a positive empirical parameter related to the adsorption capacity and n the heterogeneity factor.

2.2.4. Kinetic Models

In order to describe the mechanism of the adsorption process of BB9 onto Na-Kc, three kinetic models, pseudo-first-order, pseudo-second-order and Intraparticle diffusion were used for comparison with experimental data. Their non-linear forms are given by Eqs. (6)-(8) respectively.

$$q_t = q_e \left[1 - \exp^{(-k_1 t)}\right] \quad (6)$$

$$q_t = \frac{q_e^2 k_2 t}{1 + q_e k_2 t} \quad (7)$$

$$q_t = K_{id} t^{1/2} + \gamma \quad (8)$$

Where q_e (mg/g) and q_t (mg/g) are the quantities of BB9 dye adsorbed at the equilibrium and at time t respectively; k_1 (min^{-1}), k_2 (g/mg.min) and k_{id} ($mg/gmin^{0.5}$) are the kinetic constants of the 1st order, 2nd order and intra-particle diffusion kinetic constant respectively. γ (mg/g) is associated to the boundary layer thickness, t (min) is the time.

2.2.5. Validity of the Isotherm and the Kinetic Models

The validity of different models was evaluated using correlation coefficient (R^2) and Chi-square test (χ^2) given by the following Eqs. (9) and (10). The best fitting and similarity of a model with experimental data is decided by largest value of R^2 (or smallest values of χ^2). [18,19]

$$R^2 = 1 - \frac{\sum_{k=1}^{n} (v_{exp,k} - v_{pred,k})^2}{\sum_{k=1}^{n} (v_{pre,j} - \hat{v}_{exp})^2} \quad (9)$$

$$\chi^2 = \sum_{j=1}^{j} \frac{(v_{exp,j} - v_{pre,j})2}{\hat{v}_{exp,j}} \quad (10)$$

Where: $v_{exp,j}$ and $v_{pre,j}$ are the experimental and the predicted values of the " j^{th} " test, $\hat{v}_{exp}$ is the average experimental value.

3. Results and Discussion

3.1. pH Zero Point Charge

Figure. 3 showing the graph of ΔpH versus pH_i indicate that the pH_{zpc} is 9.01. For pH values greater than pH_{zpc}, the surface of the adsorbate is negatively charged and therefore suitable for the removal of cationic dyes such as BB9. Several other studies have revealed the same predictions [5,20].

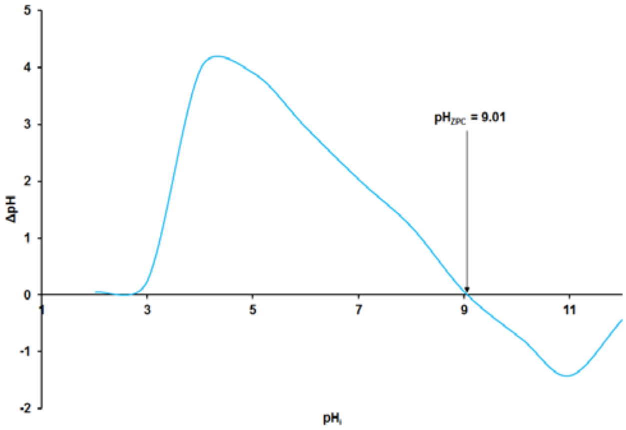

Figure 3. pH of zero-point charge (pH_{zpc}) of synthezized γ-nano alumine

In a strongly acidic environment, much lower than the pH_{ZPC}, the oxygenated surface sites of the adsorbent are protonated and carry a positive charge. In a weakly acidic environment, there is dissociation of the protonated sites of the adsorbent and formation of neutral sites. At pH_{ZPC}, the surface of the adsorbent is neutral. In a basic medium, at pH ≥ pH_{ZPC}, there is a dissociation of the surface hydroxylated functions of the adsorbent and the appearance of negatively charged sites. The surface of the adsorbent thus becomes negative.

3.2. Effect of Processing Parameters

3.2.1. Influence of Initial pH of the BB9 Solution

Figure. 4a shows the influence of initial pH on the adsorption of BB9 on Na-Kc. An increase in the percentage of elimination from 41.2% to 63.41% was observed with the initial pH of 1 to 11. The pH influences the surface charge of Na-Kc as well as the ionization of the solution. Previous work [17] indicated that for pH values increasing and above pHzpc, the surface aluminols groups (-Al-OH) of Na-Kc can react with the hydroxide ions in solution and gain negative charges. These considerations are presented by the following Eqs. (11)-(13) [19,21,22,23]

$$\text{- pH} \le pH_{ZPC} \quad Al\text{-}OH + H_3O^+ \rightleftharpoons Al\text{-}OH_2^+ + H_2O \quad (11)$$

$$\text{- pH} = pH_{ZPC}: \quad Al\text{-}OH_2^+ \rightleftharpoons AlOH + H^+ \quad (12)$$

$$\text{- pH} \ge pH_{ZPC}: \quad Al\text{-}OH + OH^- \rightleftharpoons Al\text{-}O^- + H_2O \quad (13)$$

Indeed, at higher pH, the surface has a high negative charge density. Such conditions are favorable to the uptake of positively charged BB9 due to electrostatic attraction. A reverse phenomenon will be observed if the pH decreases. A similar trend was observed by other workers for the adsorption of cationic dye on various materials [5,24,25,26].

3.2.2. Influence of Initial Concentration

The plot of the influence of the initial concentration of the adsorption of BB9 onto Na-Kc is given in Figure. 4b. The result shows that the adsorption capacity of Na-Kc increases with higher concentrations of dye. It is due to a large number of collisions between the pollutant and the adsorbent. That increase may be also due to the availability of several active sites available on the adsorbent surface, i.e. several of these sites are not occupied by the adsorbate molecules [18,22].

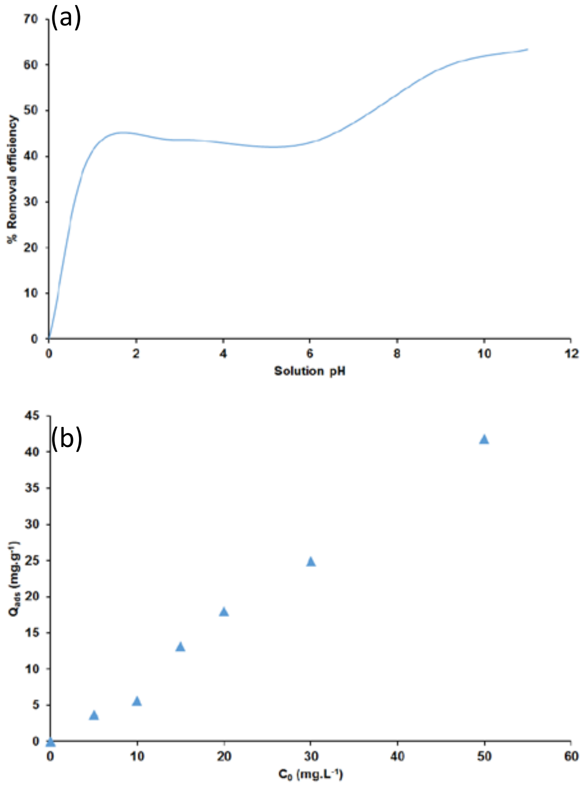

Figure 4. Plot of the influence of (a) initial pH and (b) initial concentration (V= 20 mL; T = 25±3 °C; m = 20 mg)

3.2.3. Influence of the Na-Kc's dose

The results presented in Figure 5a show that the percent removal of BB9 increases rapidly from 56 to 76.24 % when the adsorbent dose shifts from 1 to 5 g/L. In fact, the larger the mass of the adsorbent used, greater the availability of more adsorption sites and more surface area [26,27].

3.2.4. Effect of the Contact Time

The effect of contact time at an initial concentration of 50 $mg.L^{-1}$ is shown in Figure 5b. The amount of dye adsorbed increases with increasing contact time. There is a rapid adsorption of BB9 in the first 15 min followed by the gradual increase of adsorption rate and ultimately reaching saturation. The initial rapid phase may be due to abundant vacant sites of the adsorbent at the initial stage [24,27]. The steady step is due either to the saturation of those sites or the drop of BB9 concentration. These results are similar to the adsorption of dyes on different adsorbents such as: activated carbon, aerobic granules, silica-smectite composites and other adsorbents [3,28,29]. For our study, the equilibrium time chosen is 15 minutes.

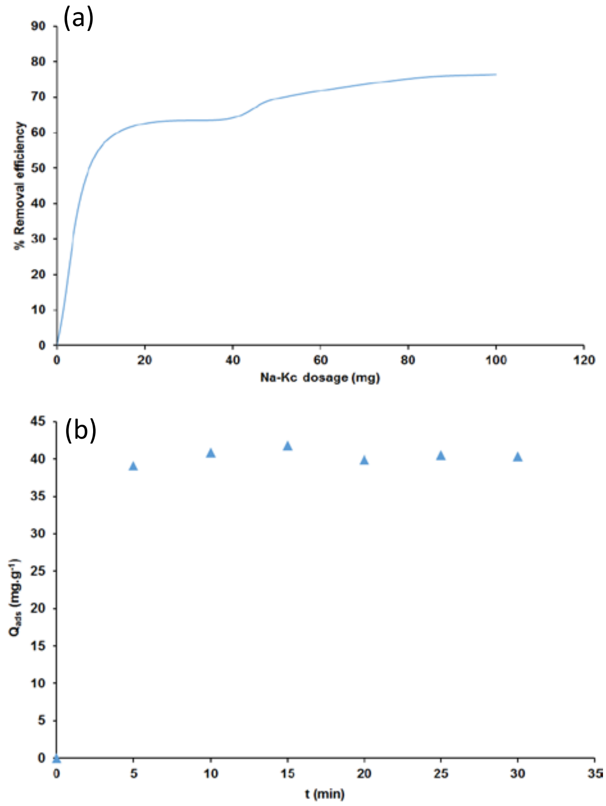

Figure 5. Influence of (a) Na-Kc dose and (b) contact time

3.3. Kinetics and Modeling Fitting

The study of the adsorption kinetics of BB9 onto Na-Kc was carried at the initial concentration of 50 mg/L, the adsorbent dose of 1g/L, and pH 11. The pseudo-first order, the pseudo-second order and intraparticle diffusion were investigated and the non-linear regressions of the models are shown on Figure 6. Table 1 presents the related kinetic parameters**.**

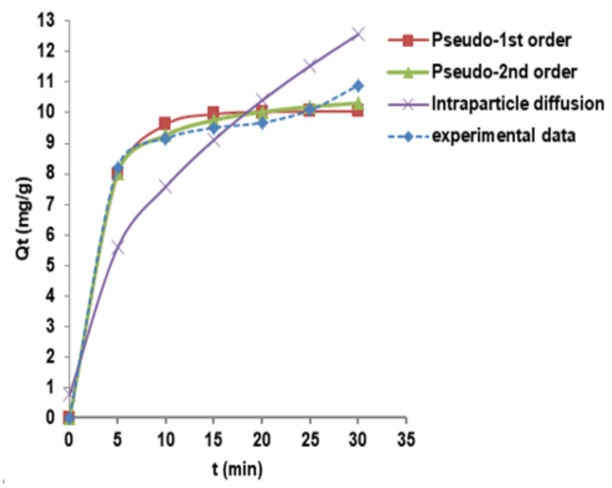

Figure 6. Plots of the non-linear kinetic models of pseudo-ordre 1; pseudo-ordre 2 and Intraparticle diffusion against the experimental data

Table 1. Non-linear kinetic parameters of BB9 adsorption onto Na-Kc

Model	Kinetic contants	
Pseudo-1st order	q_{cal} (mg.g^{-1})	10.04
	q_{exp} (mg.g^{-1})	10.90
	k_1 (min^{-1})	0.31
	R^2	0.98
	χ^2	0.13
Pseudo-2nd-order	q_{cal} (mg.g^{-1})	10.94
	q_{exp} (mg.g^{-1})	10.90
	k_2 (g.mg^{-1}.min^{-1})	0.05
	R^2	0.99
	χ^2	0.06
Intraparticle diffusion	q_{cal} (mg.g^{-1})	12.57
	q_{exp} (mg.g^{-1})	10.90
	k_{id} (mg.g^{-1}.min^{-1})	2.16
	γ (mg.g^{-1})	0.76
	R^2	0.84
	χ^2	

It was observed that for the studied conditions, the pseudo-second-order accurately predicts the adsorption kinetics with the highest determination coefficient R^2 and lowest value of χ^2. Futhermore, the experimental adsorption capacity Q_{exp} is closer to the calculated or predicted one Q_{cal}. Similar results are found in the literature for BB9 adsorption on other adsorbents [2,7].

3.4. Equilibrium Studies and Isotherms

Figure 7. presented the non-linear regression of Langmuir and Freundlich isotherms and the related equilibrium constants are presented in Table 2.

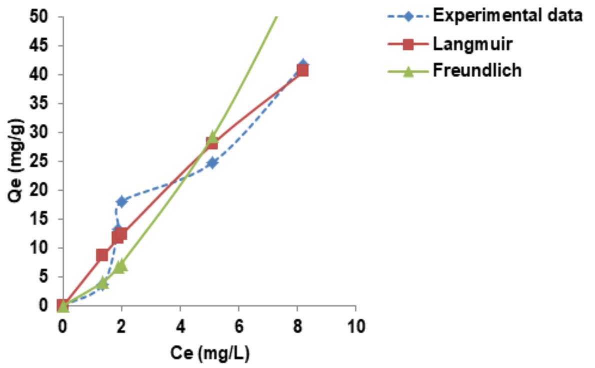

Figure 7. Nonlinear plots of the equilibrium models of Langmuir; Freundlich data against the experimental data

Table 2. The equilibrium constants of BB9 adsorption onto Na-Kc.

Model	Equilibrium constants	
Langmuir	Q_m (mg.g^{-1})	152.80
	Q_{exp} (mg.g^{-1})	41.79
	K_L (L.mg^{-1})	0.04
	R_L	0.31
	R^2	0.91
	χ^2	6.12
Freundlich	Q_{exp} (mg.g^{-1})	41.79
	K_F (mg.g^{-1})	2.62
	$\boldsymbol{n}$ (g.mg^{-1}.min^{-1})	0.676
	R^2	0.40
	χ^2	28.57

The correlation coefficients shown in Table 2 indicate that the Na-Kc-BB9 systems can be described by Langmuir isotherm given the higher correlation coefficient R^2 (0.91) and lowest value of χ^2. The good correlation with the Langmuir model assumes the formation of a monolayer on the surface of the adsorbent, all the adsorption sites are almost equivalent and therefore isoenergetic [23,30,31]. The parameter 1/n provides information on the adsorption intensity and also indicates the relative distribution of energetic sites for adsorption and depends on both the nature and strength of the adsorption process. If the value of 1/n is equal to 1, the adsorption is linear; if it is greater than 1, the adsorption is physical; if it is less than 1, adsorption is a favorable chemical process [32,33]. In our case, the value of 1/n is greater than 1(1.48) assumed that the adsorption is physical. The equilibrium parameter R_L, represents the nature of the adsorption phenomenon, which can be favorable ($0 < R_L < 1$), linear ($R_L = 1$), unfavorable ($R_L > 1$) or irreversible (R_L=0) [34,35]. The adsorption phenomenon is favorable according to the value of R_L (0.31) obtained (Table 2).

3.5. Mechanism of BB9 Adsorption onto Na-Kc Surface

The adsorption ability of alumina towards organic compounds might be influenced by several factors among which the pH of the solution and the physicochemical properties of adsorbent. The process involves Lewis acidity–basicity interaction as the ability to electron acceptation–attraction [36]. Adsorption of positively charged molecules of BB9* on the alumina surface in aqueous milieu might be considered to be a Lewis acid-base reaction. The sulfure ion S^+ on BB9 an electron acceptor and the oxygen ion O^{2-} of hydroxyl ions presented on negatively charged alumina surface, its donor. Weak S-O-Al bridges are then formed on the Na-Kc surface limited by the steric hindrance of BB9* molecules. These interactions are favorable when the surface of Na-Kc is negatively charged (pH > pH_{ZPC}) due to electrical interactions. The proposed mechanism is given in Figure 8.

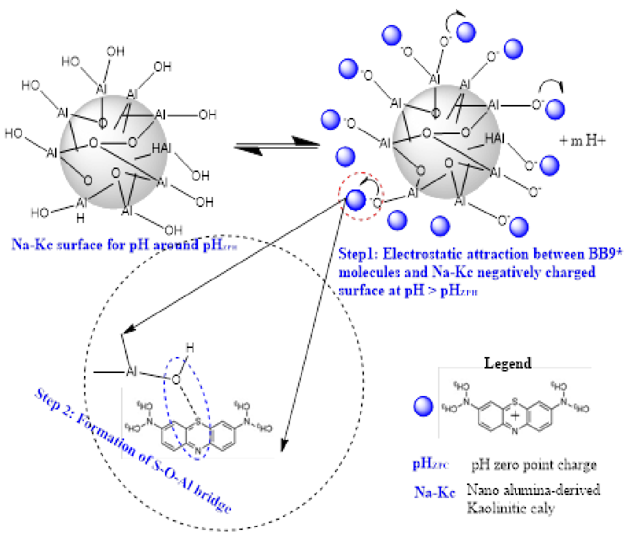

Figure 8. Proposed mechanism of the adsorption of BB9 molecules onto Na-Kc surface

The fixation of most of the dye molecules follows a two-steps mechanism. Indeed, the positively charged BB9 molecules first diffuse from the bulk solution towards the negative surface of Na-Kc due to attractive electric forces. Secondly, the fixation of dye molecules by interactions between the electrophile sites of the dye and the donor Oxygen atoms of the adsorbent forming S-O-Al bridges as illustrated on the mechanism.

Table 3 displays a comparative value of the maximum monolayer adsorption of BB9 onto various adsorbents found in the literature.

Table 3. Comparative values of maximum percent removal for BB9 adsorption of onto various adsorbents

Adsorbent	Temperature/contact time /Adsorbent dose /initial dye concentration	Maximum Adsorption Capacities (mg/g)	References
Low-Cost Natural Jordanian Tripoli	25 °C / 120 min / 5g/L / 100 mg/L	21.1	[37]
Natural Saudi red clay	25 °C / 60 min / 6g/L /100 mg/L	50.25	[32]
Kaolinite derived nanosilica	23 °C / 15 min / 1 g/L /50 mg/L	13.8	[5]
α-Chitin nanoparticles	25 °C / 30 min / 1.5 g/L /10 mg/L	82.6	[38]
Nano alumina from kaolinitic clay	25 °C / 15 min / 1g/L / 50 mg/L	41.8	Present work
Orysa sativa-derived nano silica doped smectic clay	25 °C / 50 min / 0.5 g/L / 30 mg/L	36.6	[19]
Alumina nanoparticle with SDS modification	27 °C / 120 min / 5 g/L / 48 mg/L	165	[39]
Kaolinite	30 °C / 80 min / 3 g/L / 90 mg/L	50.25	[40]

According to the Table 3, the γ-nano alumina used in this work demonstrated BB9 adsorption with similar or more efficiency compared to many others adsorbents found in the literature and with a relatively low contact time. This might be due to its nanoscale particle size and interesting specific surface area. Furthermore, the nano alumina might be of great economical interest since it is obtained from available clay material.

4. Conclusion

In this work, γ-nano alumina labeled Na-kc previously synthesized using preheated kaolinitic clay was used to adsorb dye Blue Basic 9 from aqueous solutions. Main adsorption parameters as initial concentration, initial pH, contact time and adsorbent dose were investigated to optimize the process. It was found that the initial pH of the solution is a very significant factor. The surface charge of the adsorbent depends on pH and therefore influences the speed and the type of interaction between the adsorbent and the BB9 molecules. The best conditions are pH = 11, 1g/L for adsorbent dose, 50 mg/L for initial concentration and 15 min for contact time. These led to an adsorption rate of more than 83.6%. The adsorption mechanism of BB9 is mostly controlled by electrostatic interactions in the first step followed by a tendency to form Lewis-acid interactions in the second step. Comparison with some existing adsorbents has shown that γ-nanoalumina obtained in the present study could be a good and economical alternative for the treatment of BB9 dye polluted waters.

Conflicts of Interest Statement

All authors certify that they have no affiliations with or involvement in any organization or entity with any financial interest or non-financial interest in the subject matter discussed in this manuscript.

References

[1] Al-Gheethi AA, Azhar QM, Senthil Kumar P, et al (2022) Sustainable approaches for removing Rhodamine B dye using agricultural waste adsorbents: A review. Chemosphere 287:132080.

[2] Li B, Guo J, Lv K, Fan J (2019) Adsorption of methylene blue and Cd(II) onto maleylated modified hydrochar from water. Environmental Pollution 254:113014.

[3] Kepdieu JM, Djangang CN, Njimou JR, et al (2023) Mathematical Modelling using Full Factorial Design in Response Surface Methodology Applied in the Adsorptive Removal of Dye Basic Blue 9 From Synthetic Aqueous Solutions Onto Oryza Sativa Husk-derived Nano-silica Doped Smectic Clay. In Review.

[4] Qin P, Yang Y, Zhang X, et al (2017) Highly efficient, rapid, and simultaneous removal of cationic dyes from aqueous solution using monodispersed mesoporous silica nanoparticles as the adsorbent. Nanomaterials 8: 4.

[5] Gustave T, Chantale Njiomou D, Charles Fon A, et al (2022) Nano-silica from kaolinitic clay used as adsorbent for anionic and cationic dyes removal: linear and non-linear regression isotherms and kinetics studies. Ann Civil Environ Eng 6:008–018.

[6] Santoso E, Ediati R, Kusumawati Y, et al (2020) Review on recent advances of carbon based adsorbent for methylene blue removal from waste water. Materials Today Chemistry 16:100233.

[7] Kuang Y, Zhang X, Zhou S (2020) Adsorption of Methylene Blue in Water onto Activated Carbon by Surfactant Modification. Water 12: 587.

[8] Cherifi H, Hanini S, Bentahar F (2009) Adsorption of phenol from wastewater using vegetal cords as a new adsorbent. Desalination 244: 177–187.

[9] Ighalo JO, Omoarukhe FO, Ojukwu VE, et al (2022) Cost of adsorbent preparation and usage in wastewater treatment: A review. Cleaner Chemical Engineering 3: 100042.

[10] Al-Ghouti MA, Da'ana DA (2020) Guidelines for the use and interpretation of adsorption isotherm models: A review. Journal of Hazardous Materials 393: 122383.

[11] Mor S, Chhoden K, Negi P, Ravindra K (2017) Utilization of nano-alumina and activated charcoal for phosphate removal from wastewater. Environmental Nanotechnology, Monitoring & Management 7: 15–23.

[12] Dhawale VP, Khobragade V, Kulkarni SD (2018) Synthesis and characterization of aluminium oxide (Al2O3) nanoparticles and its application in azodye decolourisation. chemistry 27: 31.

[13] Odiongenyi AO, Afangide UN (2019) Adsorption and thermodynamic studies on the removal of congo red dye from aqueous solution by alumina and nano-alumina. Communication in Physical Sciences 4.

[14] Banerjee S, Gautam RK, Jaiswal A, et al (2015) Rapid scavenging of methylene blue dye from a liquid phase by adsorption on alumina nanoparticles. RSC Adv 5: 14425–14440.

[15] Al-Rubayee WT, Abdul-Rasheed OF, Ali NM (2016) Preparation of a modified nanoalumina sorbent for the removal of alizarin yellow R and methylene blue dyes from aqueous solutions.

Journal of Chemistry 2016.

[16] Ali S, Abbas Y, Zuhra Z, Butler IS (2019) Synthesis of γ-alumina (Al 2 O 3) nanoparticles and their potential for use as an adsorbent in the removal of methylene blue dye from industrial wastewater. Nanoscale Adv 1: 213–218.

[17] Tchanang G, Kepdieu JM, Goumou K, et al (2024) Synthesis of Low-Cost ɣ-Nano Alumina-Based Kaolinitic Clay: Effect of Pre-Heating Temperature of the Precursor. MSCE 12: 108–122.

[18] Banerjee S, Gautam RK, Jaiswal A, et al (2015) Rapid scavenging of methylene blue dye from a liquid phase by adsorption on alumina nanoparticles. RSC Adv 5: 14425–14440.

[19] Kepdieu J, Djangang C, Njimou J, et al (2023) Theoretical and Experimental Study of the Adsorption of Natural Red 4 Dye from Synthetic Aqueous Media Using a Low-cost Silica-smectite Composite. AJPS 1: 1–22.

[20] Vučurović VM, Razmovski RN, Miljić UD, Puškaš VS (2014) Removal of cationic and anionic azo dyes from aqueous solutions by adsorption on maize stem tissue. Journal of the Taiwan Institute of Chemical Engineers 45: 1700–1708.

[21] Lékéné RBN, Nsami JN, Rauf A, et al (2018) Optimization Conditions of the Preparation of Activated Carbon Based Egusi (<i>Cucumeropsis mannii</i> Naudin) Seed Shells for Nitrate Ions Removal from Wastewater. AJAC 09: 439–463.

[22] Tabi GA, Blaise LNR, Daouda K, et al (2022) Non-linear modelling of the adsorption of Indigo Carmine dye from wastewater onto characterized activated carbon/volcanic ash composite. Arabian Journal of Chemistry 15: 103515.

[23] Tchanang G, Djangang CN, Abi CF, et al (2022) Nano-silica from kaolinitic clay used as adsorbent for anionic and cationic dyes removal: Linear and non-linear regression isotherms and kinetics studies. Annals of Civil and Environmental Engineering 6: 008–018.

[24] Hameed BH, Krishni RR, Sata SA (2009) A novel agricultural waste adsorbent for the removal of cationic dye from aqueous solutions. Journal of Hazardous Materials 162: 305–311.

[25] Kifuani KM, Kifuani Kia Mayeko A, Noki Vesituluta P, et al (2018) Adsorption d'un colorant basique, Bleu de Méthylène, en solution aqueuse, sur un bioadsorbant issu de déchets agricoles de Cucumeropsis mannii Naudin. Int J Bio Chem Sci 12: 558.

[26] Sumanjit, Rani S, Mahajan RK (2016) Equilibrium, kinetics and thermodynamic parameters for adsorptive removal of dye Basic Blue 9 by ground nut shells and Eichhornia. Arabian Journal of Chemistry 9: S1464–S1477.

[27] Al-Mahmoud S (2020) Kinetic and Thermodynamic Studies for the Efficient Removal of Methylene Blue Using Hordeum Murinum as a New Biosorbent. Egypt J Chem 0: 0–0.

[28] Baccini A, Laporte N, Goetz S, et al (2008) A first map of tropical Africa's above-ground biomass derived from satellite imagery. Environmental Research Letters 3: 045011.

[29] Errais E (2011) Réactivité de surface d'argiles naturelles: Etude de l'adsorption de colorants anioniques.

[30] Lekene RBN, Kouotou D, Ankoro NO, et al (2021) Development and tailoring of amino-functionalized activated carbon based Cucumerupsi manni Naudin seed shells for the removal of nitrate ions from aqueous solution. Journal of Saudi Chemical Society 25: 101316.

[31] Tabi GA, Blaise LNR, Daouda K, et al (2022) Non-linear modelling of the adsorption of Indigo Carmine dye from wastewater onto characterized activated carbon/volcanic ash composite. Arabian Journal of Chemistry 15: 103515.

[32] Khan MI (2020) Adsorption of methylene blue onto natural Saudi Red Clay: isotherms, kinetics and thermodynamic studies. Mater Res Express 7:055507.

[33] Meili L, Lins P, Costa M, et al (2019) Adsorption of methylene blue on agroindustrial wastes: experimental investigation and phenomenological modelling. Progress in biophysics and molecular biology 141: 60–71.

[34] Errais E, Duplay J, Darragi F, et al (2011) Efficient anionic dye adsorption on natural untreated clay: Kinetic study and thermodynamic parameters. Desalination 275: 74–81.

[35] Omodele EA, Adewale AG, Mikaila MM, Joshua IO (2019) A mini-review on the application of alumina nanoparticles for water treatment. 2019 FUOYE 8: 4

[36] Kasprzyk-Hordern B (2004) Chemistry of alumina, reactions in aqueous solution and its application in water treatment. Advances in Colloid and Interface Science 110: 19–48.

[37] ALzaydien AS (2009) Adsorption of Methylene Blue from Aqueous Solution onto a Low-Cost Natural Jordanian Tripoli. American J of Environmental Sciences 5: 197–208.

[38] Dhananasekaran S, Palanivel R, Pappu S (2016) Adsorption of Methylene Blue, Bromophenol Blue, and Coomassie Brilliant Blue by α-chitin nanoparticles. Journal of Advanced Research 7: 113–124.

[39] Chu T, Nguyen N, Vu T, et al (2019) Synthesis, Characterization, and Modification of Alumina Nanoparticles for Cationic Dye Removal. Materials 12: 450.

[40] Khan TA, Dahiya S, Ali I (2012) Use of kaolinite as adsorbent: Equilibrium, dynamics and thermodynamic studies on the adsorption of Rhodamine B from aqueous solution. Applied Clay Science 69: 58–66.